

**Structure, Volume 25**

## **Supplemental Information**

### **The Tetrameric Plant Lectin BanLec Neutralizes**

### **HIV through Bidentate Binding**

### **to Specific Viral Glycans**

**Jonathan T.S. Hopper, Stephen Ambrose, Oliver C. Grant, Stefanie A. Krumm, Timothy M. Allison, Matteo T. Degiacomi, Mark D. Tully, Laura K. Pritchard, Gabriel Ozorowski, Andrew B. Ward, Max Crispin, Katie J. Doores, Robert J. Woods, Justin L.P. Benesch, Carol V. Robinson, and Weston B. Struwe**

## ***Supplemental Information***

# **The tetrameric plant lectin BanLec neutralises HIV through bidentate binding to specific viral glycans**

Jonathan T.S. Hopper<sup>a</sup>, Stephen Ambrose<sup>a</sup>, Oliver C. Grant<sup>b</sup>, Stefanie A. Krumm<sup>c</sup>,  
Timothy M. Allison<sup>a</sup>, Matteo T. Degiacomi<sup>a</sup>, Mark D. Tully<sup>d</sup>, Laura K. Pritchard<sup>e</sup>, Gabriel  
Ozorowski<sup>f</sup>, Andrew B. Ward<sup>f</sup>, Max Crispin<sup>e</sup>, Katie J. Doores<sup>c</sup>, Robert J. Woods<sup>b</sup>,  
Justin L.P. Benesch<sup>a</sup>, Carol V. Robinson<sup>a</sup>, & Weston B. Struwe<sup>a,e\*</sup>

<sup>a</sup> *Department of Chemistry, Physical & Theoretical Chemistry Laboratory, University of Oxford, Oxford, OX1 3QZ, UK.*

<sup>b</sup> *Complex Carbohydrate Research Center and Department of Biochemistry, 315 Riverbend Road, University of Georgia, Athens, GA 30602, USA.*

<sup>c</sup> *Department of Infectious Diseases, King's College London, London SE1 9RT, UK.*

<sup>d</sup> *Diamond Light Source B21, Harwell Science and Innovation Campus, Didcot, OX11 0DE, UK.*

<sup>e</sup> *Department of Biochemistry, Oxford Glycobiology Institute, University of Oxford, Oxford, OX1 3QU, UK.*

<sup>f</sup> *Department of Integrative Structural and Computational Biology, CHAVI-ID, IAVI Neutralizing Antibody Center & Collaboration for AIDS Vaccine Discovery (CAVD), The Scripps Research Institute, La Jolla, CA 92037, USA.*

\*Lead Contact: weston.struwe@bioch.ox.ac.uk

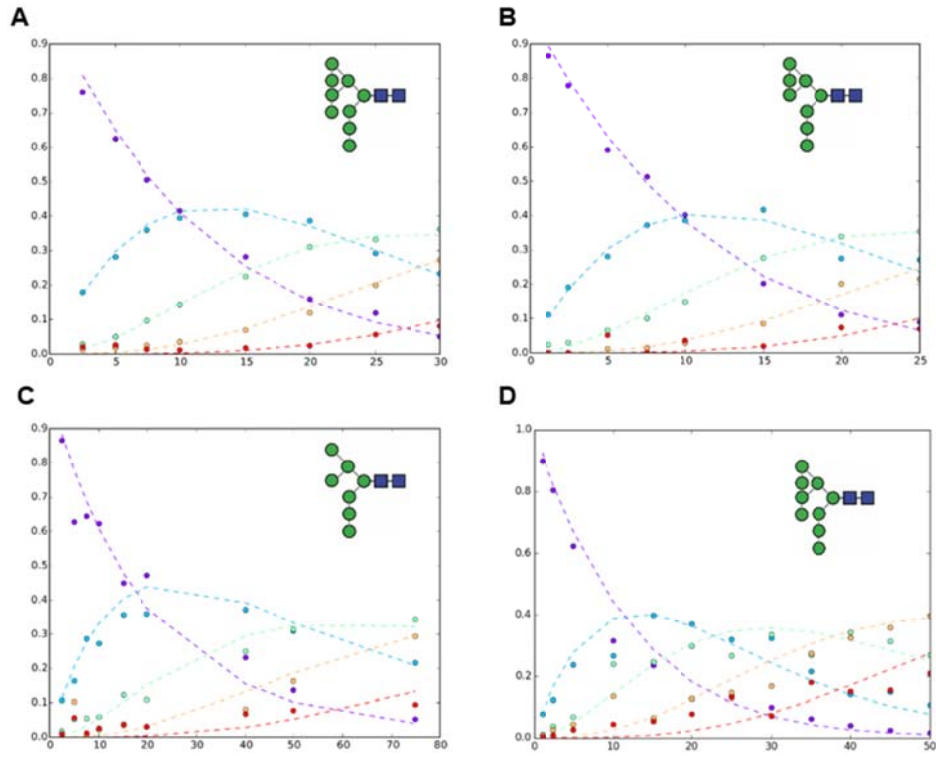


**Figure S1 (related to Figure 1):** Fits generated for the binding interactions between wild-type BanLec with Man9 (A), Man8 (B), Man7 (C); and H84T BanLec with Man9 (D). Each data point is the summed intensity for each species on a relative scale, i.e. the mole fraction. Abundances for the different BanLec tetramer:glycan stoichiometries 1:0 (purple), 1:1 (blue), 1:2 (green), 1:3 (yellow), 1:4 (red) are shown. In all cases, the y-axis = mole fraction, x-axis = BanLec concentration ( $\mu\text{M}$ )

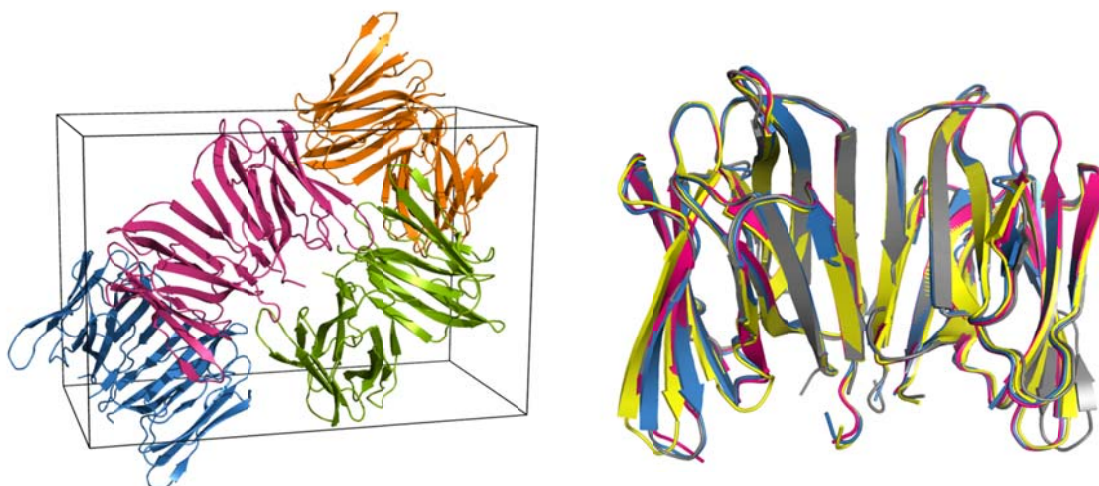


**Figure S2 (related to Figure 4):** Left: The asymmetric unit of our BanLec structure contains a dimer, and the unit cell contains four copies of the dimer, each coloured independently. The packing of the dimers in the crystal yields a tetrameric arrangement, where the interaction of each dimer is offset (e.g. the pink and green dimers). Right: A superposition using alpha-carbon positions of our BanLec structure (grey) with previously published structures shows near identical dimeric conformations between the different crystallisation conditions. Our dimer aligns with a backbone RMSD of 0.475 Å versus PDB 2BMY (blue), 0.477 Å versus PDB 3MIT (pink), and 0.464 Å and 0.505 Å for 4PIF dimers chain A and B (yellow), and chain C and D.

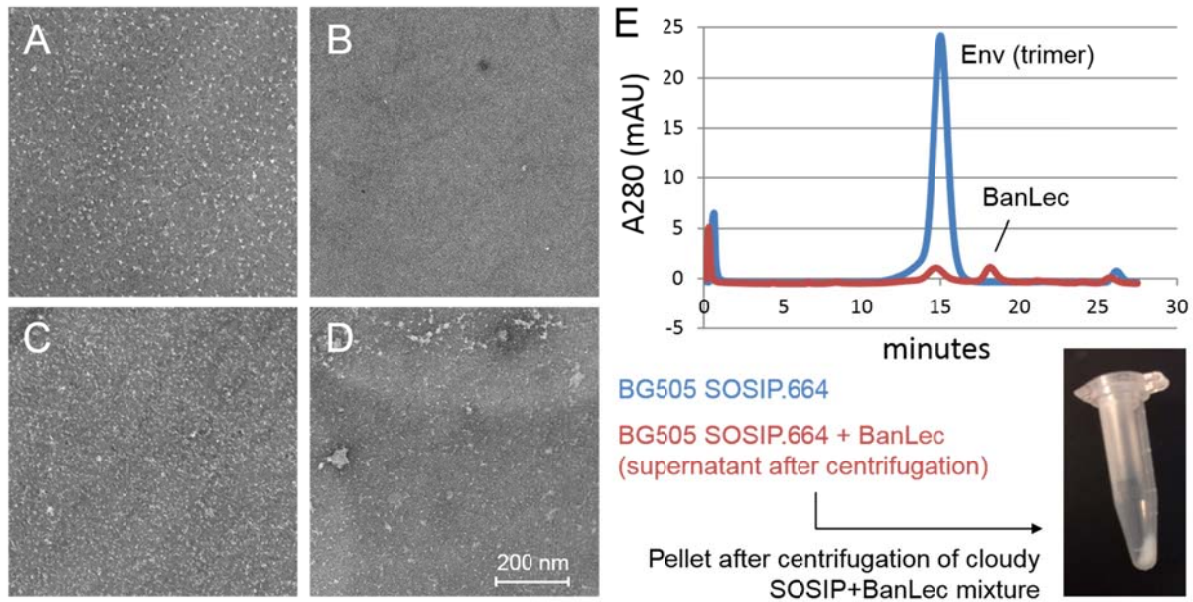


**Figure S3 (related to Figure 4):** Negative stain electron micrographs of HIV BG505 SOSIP trimers at 0.07 mg/mL (A) and in the presence of three-fold molar excess of BanLec (B). BG505 SOSIP trimer at 0.7 mg/mL (C) and in the presence of three-fold molar excess of BanLec (D). High particle density is observed in 0.7 mg/ml (roughly 20-fold typical concentration for SOSIP reconstruction), and aggregates are visible when BanLec was added. (E) Size exclusion chromatography of BG505 SOSIP trimer with and without BanLec showing gp120 aggregation, as evidenced by precipitation (lower panel), following the addition of the lectin.

<b>Site 1</b>		<b>Site 2</b>	
Residue	$\Delta G^*$	Residue	$\Delta G^*$
Protein			
K130	-4.0	D38	-3.0
D133	-3.6	D35	-2.9
F131	-2.0	G34	-2.4
G129	-2.0	V36	-1.6
G15	-1.4	T61	-0.9
H84	-1.0	Y83	-0.8
S16	-0.8	G60	-0.7
A86	-0.8	S33	-0.6
G14	-0.6	F131	-0.5
<b>Total</b>	<b>-16.3</b>	<b>Total</b>	<b>-13.5</b>
Glycan			
Man+1	-1.4	Man+1	-3.8
Man 0	-14.5	Man 0	-13.7
Man -1	+1.0	Man -1	-1.0
<b>Total</b>	<b>-15.0</b>	<b>Total</b>	<b>-18.5</b>
Protein & Glycan			
<b>Total</b>	<b>-31.1</b>	<b>Total</b>	<b>-32.0</b>

\* $\Delta G$  = estimated binding free energy (kcal mol<sup>-1</sup>), excluding solute entropy (MM-GBSA).

**Table S1 (related to Figure 5):** An MM-GBSA calculation of the per-residue binding contribution of the Man $\alpha$ 1-2Man $\alpha$ 1-3Man $\alpha$  trisaccharides in both sites of the BanLec monomer.

**Table S2 (related to Figure 5):** An MM-GBSA calculation of the per-residue binding contribution for the seven bidentate modes of Man9 with the BanLec monomer. Single point mutants that were identified for glycan binding experiments by native MS are highlighted in bold. Arrow origin indicates glycan residue bound to carbohydrate binding site II with the end point showing the second residue in carbohydrate binding site I.

g - j		g - k		g - h		g - i		j - g		i - g		i - k	
Residue	$\Delta G^*$	Residue	$\Delta G^*$	Residue	$\Delta G^*$	Residue	$\Delta G^*$	Residue	$\Delta G^*$	Residue	$\Delta G^*$	Residue	$\Delta G^*$
<b>F131</b>	-3.8	K130	-3.0	<b>F131</b>	-3.7	K130	-3.3	K130	-3.4	<b>F131</b>	-4.1	<b>D38</b>	-5.0
Y83	-3.5	<b>F131</b>	-2.6	K130	-3.5	<b>F131</b>	-3.0	<b>F131</b>	-3.0	Y83	-3.9	<b>F131</b>	-5.0
D35	-3.2	G34	-2.3	<b>H84</b>	-2.6	<b>H84</b>	-2.9	D35	-2.4	K130	-3.6	K130	-4.6
K130	-3.0	<b>D133</b>	-2.1	<b>D133</b>	-2.4	<b>D38</b>	-2.8	<b>D38</b>	-2.4	G34	-2.3	G34	-2.3
<b>H84</b>	-2.3	G129	-1.9	<b>D38</b>	-2.3	G34	-2.3	<b>H84</b>	-2.2	<b>H84</b>	-2.2	G129	-2.0
G129	-2.1	<b>H84</b>	-1.8	G34	-2.2	G129	-1.9	G129	-2.0	G129	-1.9	<b>H84</b>	-2.0
<b>D133</b>	-2.1	Y83	-1.7	G129	-1.7	D35	-1.8	G34	-1.9	<b>D133</b>	-1.8	D35	-2.0
G34	-2.1	<b>D38</b>	-1.6	V36	-1.7	<b>D133</b>	-1.8	<b>D133</b>	-1.9	V36	-1.7	S58	-1.9
<b>D38</b>	-2.0	V36	-1.6	Y83	-1.4	V36	-1.6	V36	-1.6	<b>D38</b>	-1.6	<b>D133</b>	-1.7
V36	-1.9	D35	-1.4	D35	-1.4	Y83	-1.6	G15	-0.9	D35	-1.4	V36	-1.7

\* $\Delta G$  = estimated binding free energy (kcal mol<sup>-1</sup>) excluding solute entropy (MM-GBSA).

Distance restraints input file\*:

133	ASP	N	AAA	2MA	O6	4.5	5.5
133	ASP	OD1	AAA	2MA	O4	2.2	3.2
133	ASP	OD2	AAA	2MA	C6	2.5	3.5
131	PHE	O	AAA	2MA	O6	2.5	3.5
131	PHE	N	AAA	2MA	O6	2.8	3.8
130	LYS	N	AAA	2MA	O6	2.9	3.9
130	LYS	N	AAA	2MA	O5	3.2	4.2
129	GLY	CA	AAA	2MA	O2	3.3	4.3
128	GLY	O	AAA	2MA	O2	4.2	5.2
15	GLY	CA	AAA	2MA	O3	3.4	4.4
34	GLY	CA	BBB	OMA	O2	3.0	4.0
34	GLY	N	BBB	OMA	O6	2.6	3.6
35	ASP	N	BBB	OMA	O6	3.2	4.2
36	VAL	O	BBB	OMA	O6	2.7	3.7
38	ASP	N	BBB	OMA	O6	4.1	5.1
38	ASP	CG	BBB	OMA	O4	2.7	3.7

\*For each structure selected for this procedure, the values of AAA and BBB were replaced with the appropriate saccharide residue number.

**Table S3 (related to Figure 5):** Distance restraints were introduced (value1 = 0.001, value2 = 1) during the final 200 ps of equilibration. They were turned off (value1 = 1, value2 = 0.001) during the first 1 ns of production, and no restraints (value1 = 0, value2 = 0) were used for the remaining 10 ns of production.